SOILS AND FOUNDATIONS Vol. 51, No. 4, 737–747, Aug. 2011
Japanese Geotechnical Society

EFFECT OF DIRECTIONAL STRESS HISTORY ON ANISOTROPY OF INITIAL STIFFNESS OF COHESIVE SOILS MEASURED BY BENDER ELEMENT TESTS

JINHYUN CHOO[i], YOUNG-HOON JUNG[ii] and CHOONG-KI CHUNG[iii]

ABSTRACT

This paper describes the initial stiffness of reconstituted kaolinite clay in both vertical and horizontal planes under three different stress histories. The initial shear stiffness was obtained from bi-directional bender element tests during isotropic and K_0 stress loading and unloading. An empirical correlation was established based on the initial stiffness of normally consolidated soils. Unlike the unique relationship of the initial vertical stiffness of normally consolidated clays, the initial stiffness in the horizontal plane is dependent on the stress ratio and previous stress history; thus, three different relationships of the initial horizontal stiffness were obtained for the three loading programs. The effect of the stress history on the initial horizontal stiffness can be considered properly by defining the degree of overconsolidation in terms of the horizontal effective stress. The change in the initial stiffness has a directional dependency on the stress history in the direction of the particle motion and wave propagation in the bender element tests.

Key words: anisotropy, bender element test, clay, elastic shear modulus, overconsolidation, stress history (**IGC**: D6/D7/E2)

INTRODUCTION

The small-strain behavior of soils can be characterized by two essential components: the initial stiffness and the nonlinear degradation of the stiffness. Numerous studies (Gasparre et al., 2007; Jamiolkowski et al., 1995; Lings et al., 2000; Pennington et al., 1997; Viggiani and Atkinson, 1995) have been dedicated to investigating factors affecting the initial stiffness of clays. The major factors affecting the initial stiffness such as the void ratio, stress history, and current stress level can be considered by representing the initial stiffness using the well-known equation proposed by Hardin and Richart (1963);

$$G_{ij}^0 = S_{ij} f(e) \mathrm{OCR}^k (\sigma_i')^{n_i} (\sigma_j')^{n_j}, \quad (1)$$

where G_{ij}^0 is the elastic shear modulus of the *i-j* plane, OCR is the overconsolidation ratio, $f(e)$ is a function of the void ratio, S_{ij}, n_i, n_j, and k are material constants, σ_i' is the effective normal stress in the wave propagation direction, and σ_j' is the effective normal stress in the particle motion direction. As shown in Eq. (1), the power function of the OCR can reflect the effect of the vertical stress history on the initial stiffness for the overconsolidated soil, which may exhibit a minor change in the void ratio.

According to Santagata (2008), it is generally recognized that once the effects of the stress level and void ratio are considered, the initial stiffness is not dependent on the OCR. Santagata et al. (2005) suggested that only two variables, e.g., either the effective stress and void ratio or the effective stress and OCR, are required to describe the variation of the initial stiffness of reconstituted Boston Blue Clay. Even before the study of Santagata et al. (2005), similar conclusions had been made by Jamiolkowski et al. (1995) and Rampello et al. (1997).

The factors affecting the initial stiffness appear to be sufficiently investigated; however, the conclusion with regard to the initial stiffness must be taken with caution since it is limited to the elastic shear modulus in the vertical plane, i.e., G_{vh}^0. The majority of the testing conditions for the influencing factors were performed in the vertical plane: the resonant column tests (e.g., Hardin, 1978; Hardin and Kalinski, 2005), the measurement of wave propagation velocities under laterally confined conditions (e.g., Bellotti et al., 1996), uniaxial loading under undrained conditions (e.g., Clayton and Heymann, 1999; Santagata et al., 2005), and small amplitude cyclic loading (e.g., Hoque and Tatsuoka, 2004; Kuwano and Jardine, 2002). Due to insufficient experimental data, however, it is questionable whether some conclusions on

[i] Research Specialist, Geotechnical Engineering and Tunneling Research Division, Infrastructure Research Department, Korea Institute of Construction Technology.
[ii] Assistant Professor, Department of Civil Engineering, Kyung Hee University, South Korea (jyounghoon@khu.ac.kr).
[iii] Professor, Department of Civil and Environmental Engineering, Seoul National University.
The manuscript for this paper was received for review on July 7, 2010; approved on March 28, 2011.
Written discussions on this paper should be submitted before May 1, 2012 to the Japanese Geotechnical Society, 4-38-2, Sengoku, Bunkyo-ku, Tokyo 112-0011, Japan. Upon request the closing date may be extended one month.

the initial stiffness in the vertical plane are also valid for the initial stiffness in the horizontal plane.

When the elastic shear wave propagates and the particle moves in the horizontal direction, the initial stiffness can be expressed using the following relationship:

$$G^0_{hh} = S_{hh} f(e) \mathrm{OCR}^k (\sigma'_h)^{2n_h}, \quad (2)$$

where G^0_{hh} is the initial shear stiffness in the horizontal plane, σ'_h is the effective normal stress in the horizontal direction, and n_h is the exponent, generally equal to n_i and n_j. Equation (2) implicitly explains the characteristics of the horizontal initial stiffness. For example, the vertical effective stress has little effect on the horizontal stiffness so that Eq. (2) does not include the vertical effective stress. The soil structure in the horizontal plane represented by S_{hh} in Eq. (2) is different from S_{vh} in the vertical plane, which represents the inherent anisotropy of cohesive soil. The reduction of the void volume expressed by $f(e)$ indicates the increase of the soil density so that the wave velocity, and thus the initial stiffness increases. The implications of every component but the OCR in Eq. (2) are physically clear. The OCR represents the history of the vertical effective stress which is not explicitly relevant to the mechanical properties in the horizontal direction. If the assertion of Santagata (2008) —that the initial stiffness is not dependent on the OCR— is also valid for G^0_{hh}, the ambiguous OCR for G^0_{hh} can be simply ignored regardless of the direction of the stress in its definition. Otherwise, it is necessary to investigate how the directional stress history affects the variation of G^0_{hh}.

In this study, the effect of the directional stress history on the initial horizontal stiffness of cohesive soil is investigated. Using a stress-path controlled triaxial testing device equipped with bi-directional bender elements, both G^0_{vh} and G^0_{hh} for normally consolidated and overconsolidated soils were measured under three different loading programs: (i) isotropic stress loading and unloading, (ii) K_0 stress loading and unloading, and (iii) combined stress loading and unloading.

TESTING DEVICE AND SOIL

An automated triaxial testing system with small-strain stiffness measuring devices was used in this study. Figure 1 shows a schematic diagram of the testing system. The loading apparatus was a load frame-based triaxial testing system with automated stress path controls. Two pressure-volume controllers were used to measure and control the water pressure and volume change in the soil specimen. An internal submersible load cell with a full range of ± 4 kN and a resolution of 0.06 N was used.

Two pairs of bender elements were installed in vertical and horizontal directions to measure the anisotropic elastic shear moduli, G^0_{vh} and G^0_{hh}, using the shear wave measurements. The vertical direction bender elements were mounted in the top cap and the base platen of the triaxial test cell, and the horizontal direction bender elements were anchored in the acryl cantilevers shaped to fit the curvature of the 70 mm diameter triaxial test specimen. Local LVDTs and calipers with a full range of ± 2.5 mm and a resolution of 0.00008 mm were attached directly to the specimens to control the K_0 stress state by measuring small strains in axial and radial directions. Figure 2 shows the triaxial specimen equipped with bender elements and local LVDTs.

Reconstituted kaolinite samples were used for the

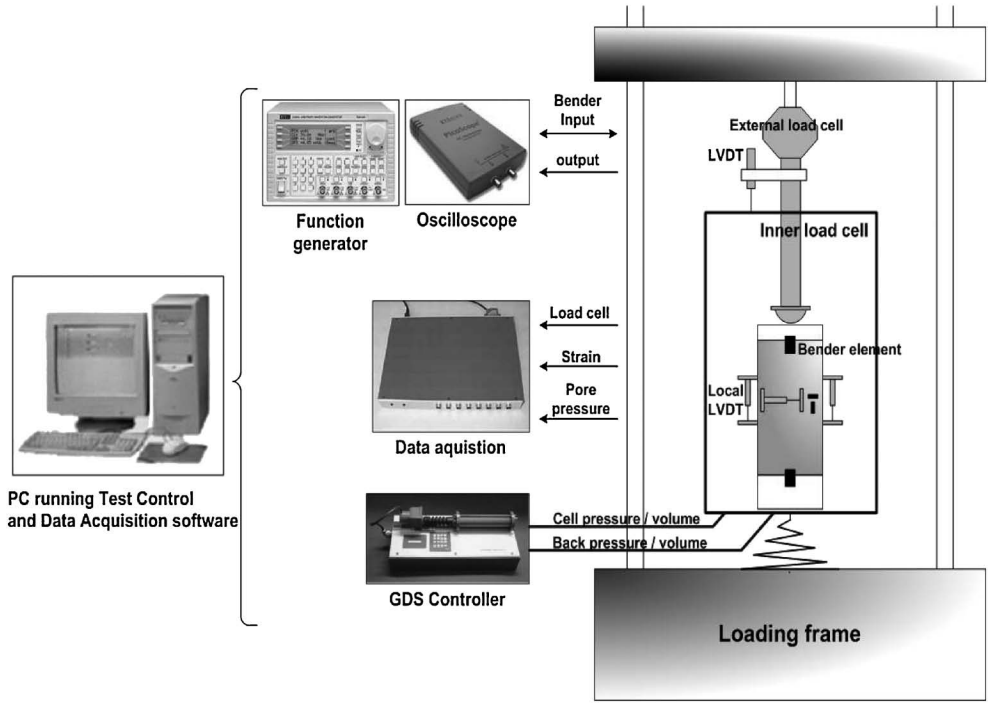

Fig. 1. Schematic diagram of the automated triaxial testing system

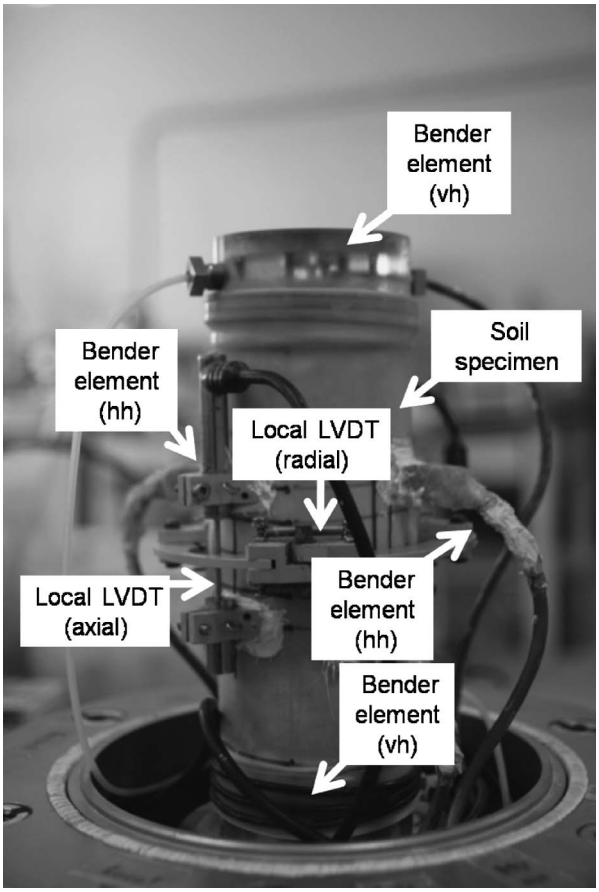

Fig. 2. Triaxial specimen equipped by the local LVDTs and bender elements

Table 1. Index properties of the reconstituted kaolinite clay

Specific gravity	2.59
Liquid limit (%)	53
Plasticity index (%)	20
Percentage finer than #200 sieve (%)	98
Initial water content (%)	45.9
Initial void ratio	1.19
Consolidation yield stress (kPa)	140 kPa
Unified soil classification system (USCS)	MH
Compression index, C_c	0.32
Recompression index, C_r	0.03

triaxial experiment. Table 1 summarizes the index properties of the reconstituted kaolinite. For the reconstitution, the kaolinite powder was initially mixed into a slurry with a water content of 110%, approximately double that of the liquid limit. To obtain the flocculated clay structure and eliminate the bacteria that may alter the chemical properties of the soil, salt of 16 g/l and NaN_3 diluted to 0.01% were added to the slurry. The kaolinite slurry was mechanically mixed in a mixing chamber. During the mixing process, the chamber was vacuumed to assist in the complete saturation of the slurry. After the slurry was completely mixed, it was placed into the consolidation chamber. To minimize possible wall friction, a 1 mm thick silicone grease layer was applied to the inner wall of the consolidation chamber. Following the sedimentation and self-weight consolidation in the consolidation chamber, the slurry was incrementally consolidated up to the vertical stress of 140 kPa. For the triaxial testing, the cylindrical specimens with dimensions of 70 mm diameter and 140 mm height were obtained from the reconstituted kaolinite block. To minimize the end friction in the triaxial specimen, lubricated ends were used for both the base platen and the top cap of the triaxial cell.

MEASUREMENT OF THE INITIAL SHEAR STIFFNESS USING BENDER ELEMENTS

During the triaxial experiments, the initial shear stiffness, G^0_{vh} and G^0_{hh}, were measured via two pairs of bender elements installed in the vertical and horizontal directions. TGA 1240 Waveform Generator (TT Instruments Ltd.) was used to generate shear waves in the bender elements. A computer aided oscilloscope, Pico technology ADC-212, received and visualized the shear waves via a computer program. Since the resonant frequency of a bender element buried in the soil mass depends on its embedded depth, two different frequencies were selected for each bender element pair: 10 kHz for the 2.25 mm element in the vertical direction, and 5 kHz for the 5 mm element in the horizontal direction based on the suggestion by Lee and Santamarina (2005).

The travel distance is one of the most important concerns for the determination of the shear wave velocity. Based on the experimental study by Viggiani and Atkinson (1995), the tip-to-tip distance was used as the travel distance of the shear wave. Because the dimension of the sample continuously changed with soil deformation, the axial and radial distances were continually updated using the measured displacements obtained from the external axial LVDT for the vertical direction and the local radial LVDT for the horizontal direction.

Determination of the arrival time of the shear wave is also crucial to measuring the shear wave velocity using bender elements. A number of methods have been suggested for the detection of the first arrival of the shear wave in bender element tests, such as first deflection, peak-to peak, cross-correlation and zero after first bump. In this study, the zero after first bump method was selected for the first arrival time of shear wave as suggested by Lee and Santamarina (2005). Figure 3 shows an example of analyzing the raw data and determining the shear wave travel time from bender element measurement.

From the wave propagation theory assuming a semi-infinite, homogeneous and elastic soil mass, the elastic shear modulus of soil can be calculated using the following equation.

$$G^0 = \rho V_s^2 \tag{3}$$

where G^0 is the initial shear modulus of the soil, ρ is the bulk density of soil, and V_s is the shear wave velocity. For the calculation of Eq. (3), the shear wave velocity was measured using the bender elements and the bulk density was calculated from the specific gravity of the soil, its

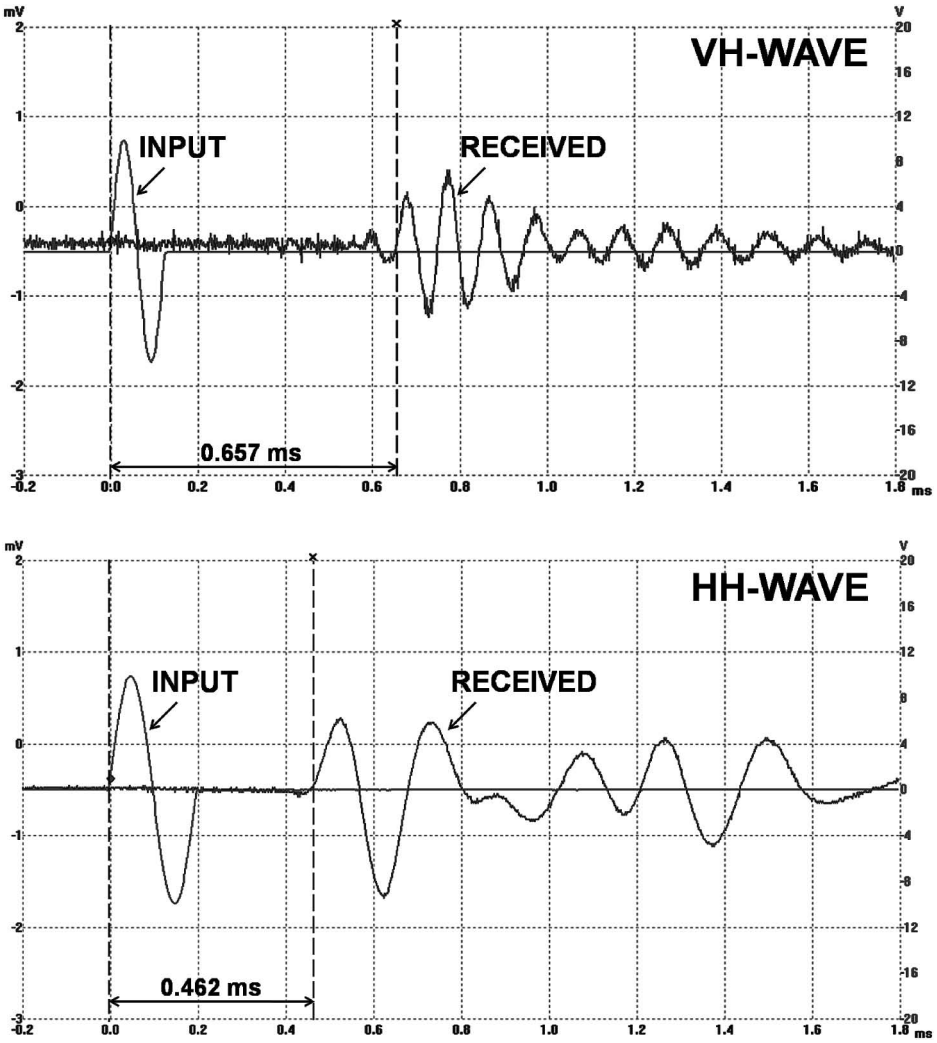

Fig. 3. Determination of the shear wave velocity in the bender element tests

Table 2. Testing Programs

Loading program	Testing stage				
	Stage 1	Stage 2	Stage 3	Stage 4	Stage 5
Isotropic stress history test	Isotropic loading until $\sigma'_v = 340$ kPa (OCR = 1)	Isotropic unloading σ'_v: 340→85 kPa (OCR: 1→4)	Isotropic reloading σ'_v: 85→480 kPa (OCR: 4→1)	Isotropic unloading σ'_v: 480→240 kPa (OCR: 1→2)	Isotropic reloading σ'_v: 240→500 kPa (OCR: 2→1)
K_0 stress history test	K_0 loading until $\sigma'_v = 340$ kPa (OCR = 1)	K_0 unloading σ'_v: 340→85 kPa (OCR: 1→4)	K_0 reloading σ'_v: 85→480 kPa (OCR: 4→1)	K_0 unloading σ'_v: 480→240 kPa (OCR: 1→2)	K_0 loading σ'_v: 240→600 kPa (OCR: 2→1)
Combined stress history test	K_0 loading until $\sigma'_v = 220$ kPa (OCR = 1)	K_0 unloading σ'_v: 220→110 kPa (OCR: 1→2)	K_0 reloading σ'_v: 110→360 kPa (OCR: 2→1)	K_0 unloading σ'_v: 360→90 kPa (OCR: 1→4)	Isotropic reloading σ'_v: 90→400 kPa (OCR: 4→1)

water content, and the void ratio.

EXPERIMENTAL PROGRAM

The experimental programs were designed to investigate the variations of G^0_{vh} and G^0_{hh} of the cohesive soil in the isotropic, K_0 stress states, and a combination of isotropic and K_0 stress states. The soil specimen was initially saturated by 250 kPa of back pressure for approximately 24 hours in order to ensure saturation. Full saturation of the specimen was subsequently accomplished by verifying that the B value was greater than 0.98.

After saturation, three loading programs were conducted: (i) an isotropic stress history test, (ii) a K_0 stress history test, and (iii) a combined stress history test. Detailed information on the loading stages of each program is provided in Table 2. Figure 4 presents the stress paths in the σ'_v-σ'_h plane. The isotropic stress history test, a typi-

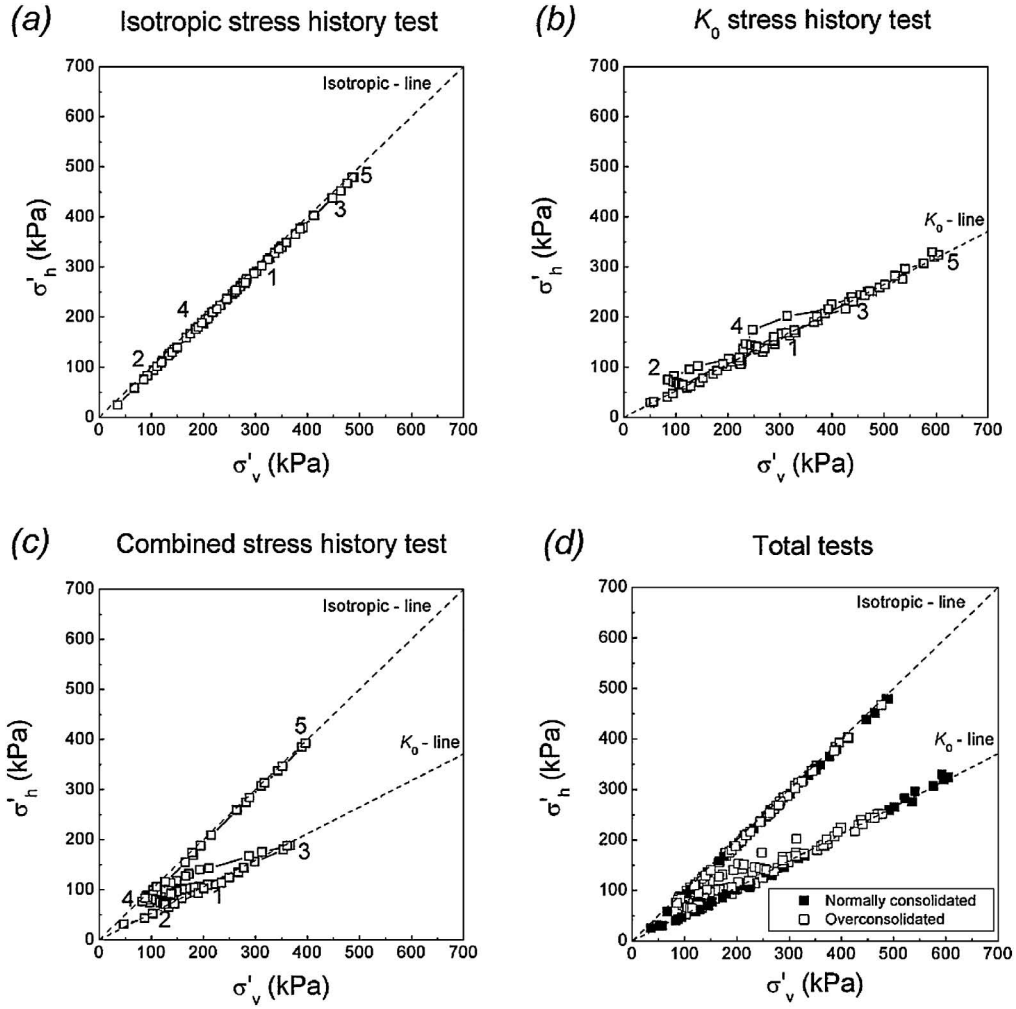

Fig. 4. Applied stress paths: (a) the isotropic stress history test, (b) K_0 stress history test, and (c) combined stress history test, (d) total tests

cal loading program for most experimental works, was chosen to measure the anisotropy of the initial shear stiffness under the isotropic stress condition. In the isotropic stress history test, there were two unloading-reloading cycles at $\sigma'_v = 340$ kPa (stage 2 and 3) and 480 kPa (stage 4 and 5) until the soil was fully loaded at $\sigma'_v = 500$ kPa (stage 5). Secondly, the K_0 stress history, a stress condition under which natural soils are likely to experience, was applied. The K_0 stress history test also involved two unloading-reloading cycles at $\sigma'_v = 340$ (stage 2 and 3) and 480 kPa (stage 4 and 5). During the K_0 unloading and reloading, the lateral stress as well as the stress ratio maintained the constraint lateral deformation of the specimen so that the stress path was not a straight line in the σ'_v-σ'_h plane. Afterwards, the specimen was loaded under K_0 condition until $\sigma'_v = 500$ kPa. The third program, the combined stress history test, was designed to investigate the effect of the previous stress history on the initial stiffness during isotropic compression. Initially, the specimen was K_0 consolidated until $\sigma'_v = 360$ kPa (stage 1 and 3) including an unloading at at $\sigma'_v = 220$ kPa (stage 2). After completion of the K_0 consolidation, the specimen was K_0 unloaded until the stresses became isotropic at $\sigma'_v = 90$ kPa (stage 4). Subsequently, the specimen was isotropically recompressed until $\sigma'_v = 400$ kPa (stage 5). Therefore, the last compression stages of the isotropic stress history test and the isotropic recompression of the combined stress history test are the same as the isotropic loading, but their previous stress histories were different.

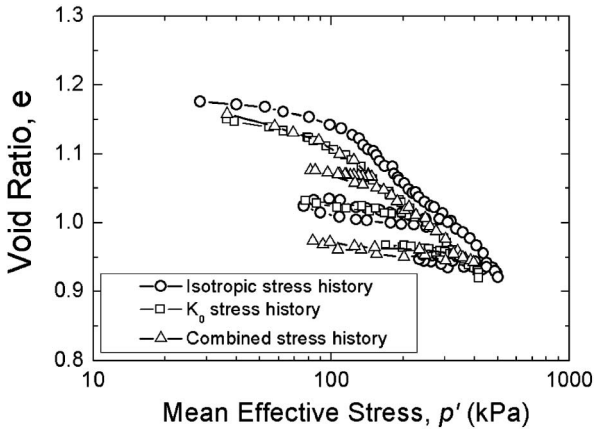

Fig. 5. Void ratio-mean effective stress relationship

The loading conditions were also separated into normally consolidated (NC) and overconsolidated (OC)

states based on the present vertical effective stress against the consolidation yield stress or the OCR value. The stress conditions of the NC and OC states in the three loading programs are presented in Fig. 4(d).

Based on the preliminary study on reconstituted kaolinite clay by Kim (2004), the loading rate of 1.5 kPa/hr in the NC state and 3.0 kPa/hr in the OC state was carefully chosen to minimize the generation of excess pore water pressure. Prior to applying each testing stage, the drained creep was imposed on the specimen for more than 30 hours until the axial strain rate of less than 0.01% /day was observed in the local strain measurement. Figure 5 shows the relationship between the void ratio and mean effective stress, $p' = (\sigma'_v + 2\sigma'_h)/3$ during the tests.

INITIAL SHEAR STIFFNESS OF NORMALLY CONSOLIDATED CLAY

To establish a reference relationship between the initial stiffness and stresses, the data from the bender element tests on normally consolidated clays were analyzed. The initial stiffness results of G^0_{vh} and G^0_{hh} are presented in Fig. 6. Regardless of the stress ratio in different loading programs, the variation of the initial stiffness, G^0_{vh}, in Fig. 6(a) is well described by a power function of the vertical and horizontal stresses. Based on Eq. (1), the regression analysis of the data of G^0_{vh} results in the expression:

$$\frac{G^0_{vh}}{p_a} = 384\left(\frac{\sigma'_v}{p_a}\right)^{0.38}\left(\frac{\sigma'_h}{p_a}\right)^{0.38} \quad (4)$$

Note that the same exponent is used for both the vertical and horizontal effective stresses normalized by p_a. The sum of the exponents is approximately 0.76, which is larger than the typical value of 0.50 for most soils (Jardine, 1995). The coefficient of determination, R^2, is shown in the figure.

The initial stiffness of soils relates to the change of the void ratio representing the variation of the soil density in shear wave propagation, as described in Eq. (2). The empirical expression of the initial stiffness in Eq. (1) accounts for the densification of soil via both the void ratio function, $f(e)$, and the power function of the stresses. However, the evaluation of each function is not straightforward because the two functions depend on each other. Higher variations of the void ratio function lead to a smaller exponent, and vice versa. According to Rampello et al. (1997), the change in the void ratio is generally dependent on the stress level so that the void ratio function may be replaced by a function of the mean normal stress. Herein, the void ratio function has been omitted in Eq. (4), which implies that a power function of the vertical and horizontal stresses implicitly accounts for the effect of the void ratio on the change in soil density and thus the initial stiffness. Accordingly, this particular choice of empirical expression without the void ratio function leads to a relatively high value of the exponent as in Eq. (4). Herein, the void ratio functions were omitted to avoid an excessive complication in expressing the relationships between the directional initial stiffnesses and stresses.

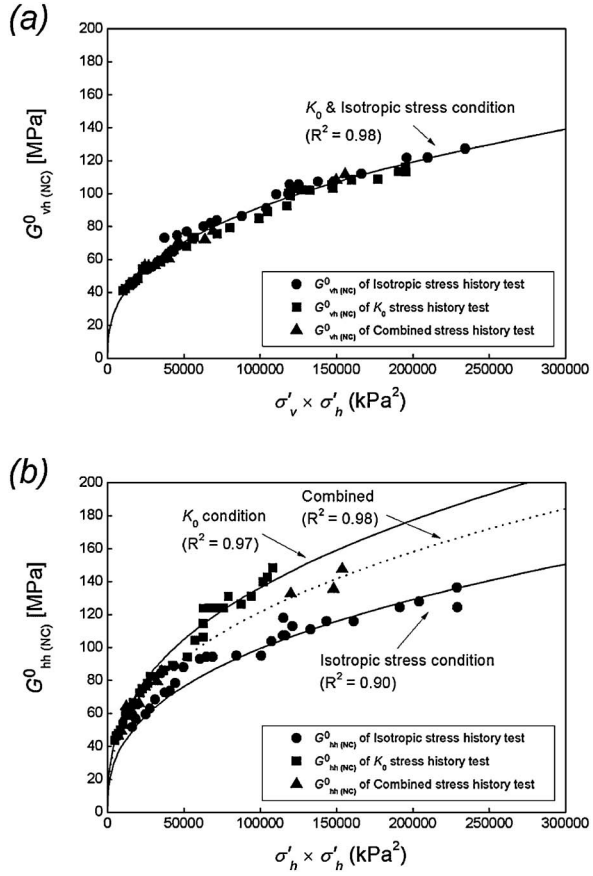

Fig. 6. Variation of the initial stiffness for normally consolidated clay: (a) G_{vh}, (b) G_{hh}

The unique relationship between G^0_{vh} and the stresses suggests that the initial stiffness in the vertical plane is not dependent on either the stress ratio or previous stress history. However, such relationship of G^0_{vh} cannot be applied to G^0_{hh}. As considered in Eq. (1), G^0_{hh} is independent of the vertical stress because both the wave propagation and polarization are towards the same horizontal direction. Therefore, if the horizontal stress does not change, the value of G^0_{hh} should remain constant for any combination of vertical and horizontal stresses. As shown in Fig. 4(b), however, the experimental data of G^0_{hh} is quite different from this expectation. For the same horizontal stress, the values of G^0_{hh} are apparently larger under K_0 stress condition than under the isotropic stress condition. Even under the same isotropic stress condition, the values of G^0_{hh} are not unique but dependent on the previous stress history because the value of G^0_{hh} for the isotropic recompression of the combined stress history test is larger than that for the isotropic stress history test.

Ignoring the minor differences in the fitted values of the exponent and using the same exponent as the value for G^0_{vh}, the regression analysis on measured values of G^0_{hh} results in the following equations:

$$\frac{G^0_{hh}}{p_a} = 569\left(\frac{\sigma'_h}{p_a}\right)^{0.76}$$

for the K_0 stress history test (5)

$$\frac{G^0_{hh}}{p_a} = 507\left(\frac{\sigma'_h}{p_a}\right)^{0.76}$$

for the combined stress history test (6)

$$\frac{G^0_{hh}}{p_a} = 415\left(\frac{\sigma'_h}{p_a}\right)^{0.76}$$

for the isotropic stress history test (7)

A similar pattern of G^0_{hh} depending on the stress ratio has also been found by Mitaritonna et al. (2008) who reported that the horizontal stiffness of reconstituted Lucera clay was more influenced by the compression stress ratio than the vertical stiffness. These experimental findings, including the current data, indicate that the empirical expression of the initial stiffness in the form of Eq. (1) may be invalid for the G^0_{hh} of cohesive soils. For cohesionless soils, however, the empirical expression of Eq. (1) predicts the relationship between G^0_{hh} and the horizontal stress. For example, Kuwano and Jardine (2002) reported that the variation of the G^0_{hh} of cohesionless soils primarily relates to the horizontal stress and is independent of previous stress histories. Herein, different forms of empirical relationships for Eqs. (5), (6) and (7) are adopted for further discussion of the initial stiffness because the current interpretation of experimental data will only be limited for these particular cases of K_0, isotropic and combined stress histories. Thus, additional studies on the dependence of G^0_{hh} on the stress ratio and stress history are necessary.

INITIAL SHEAR STIFFNESS OF OVERCONSOLIDATED CLAY

The change in the void ratio is much smaller in the overconsolidated clay than in the normally consolidated clay. For the overconsolidated clay, the degree of overconsolidation, or the overconsolidation ratio (OCR) describes the variation of the initial stiffness better than the void ratio.

In Eq. (1), the void ratio function, $f(e)$, and the power function of the OCR describe different responses in the normally consolidated and overconsolidated soils. For example, Fig. 7 compares the values obtained from the void ratio function, $f(e) = e^{-2.44}$, and the power function of the OCR, $OCR^{0.15}$, used by Santagata et al. (2005). The parameters for completing Fig. 7 were obtained from one-dimensional consolidation tests, and are provided in Table 1. As the axial stress increases under the normally consolidated condition, the value of $f(e)$ significantly increases whereas the value of the power function of the OCR remains constant because OCR = 1. As the vertical stress decreases in the overconsolidated stress region, however, the value of $f(e)$ decreases, but the value of the power function of the OCR increases. Therefore, if the initial stiffness normalized by the power function of effective stress increases as the vertical stress decreases, the OCR function should be considered regardless of the existence of the void ratio function.

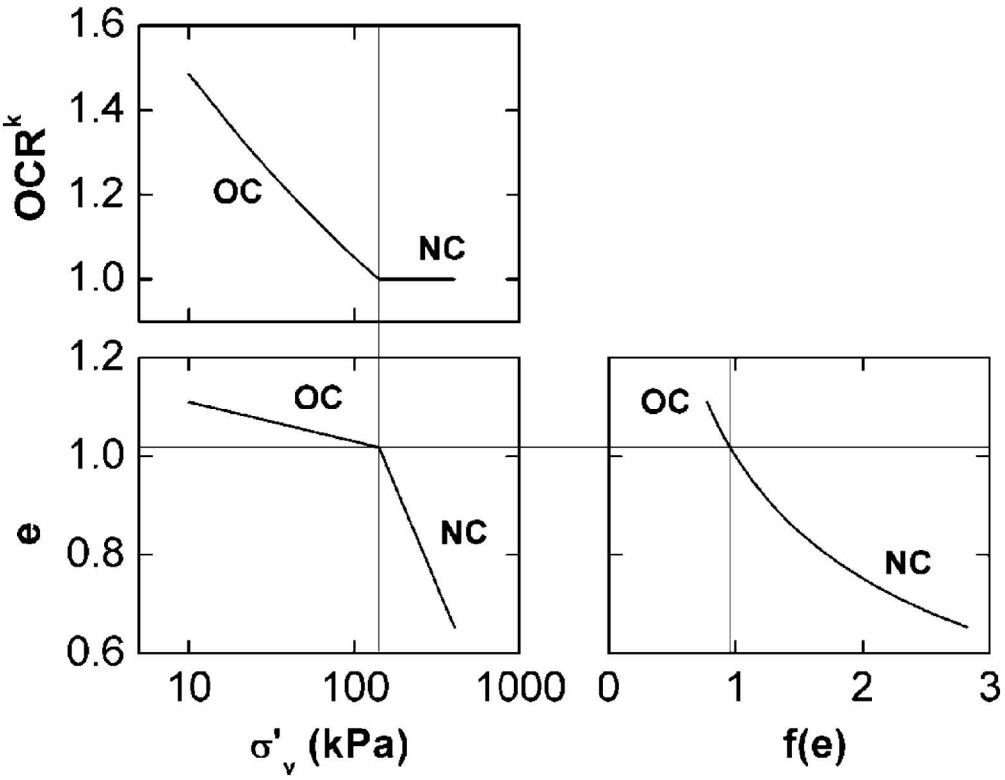

Fig. 7. Variation of the void ratio function, OCR function and e-log σ'_v relationship

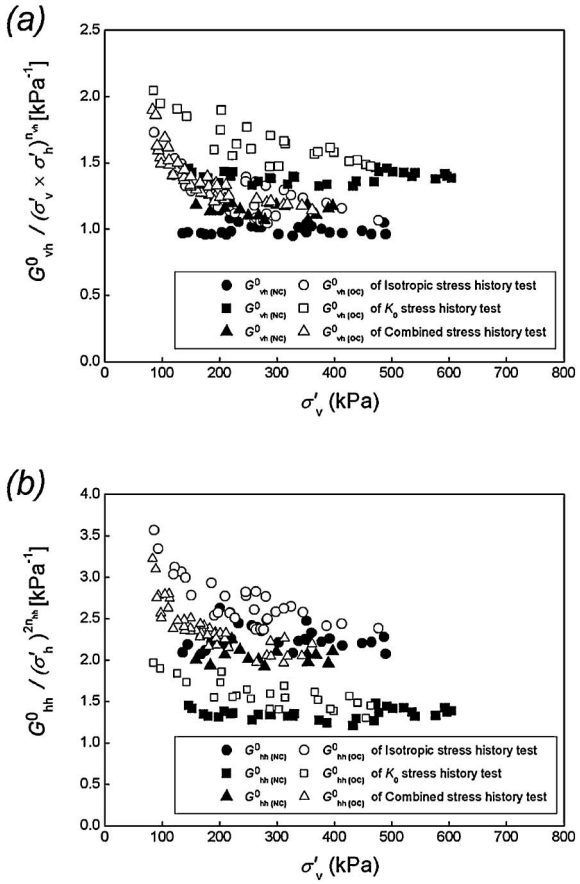

Fig. 8. The initial stiffness normalized by the power functions of the effective stresses with the vertical effective stress

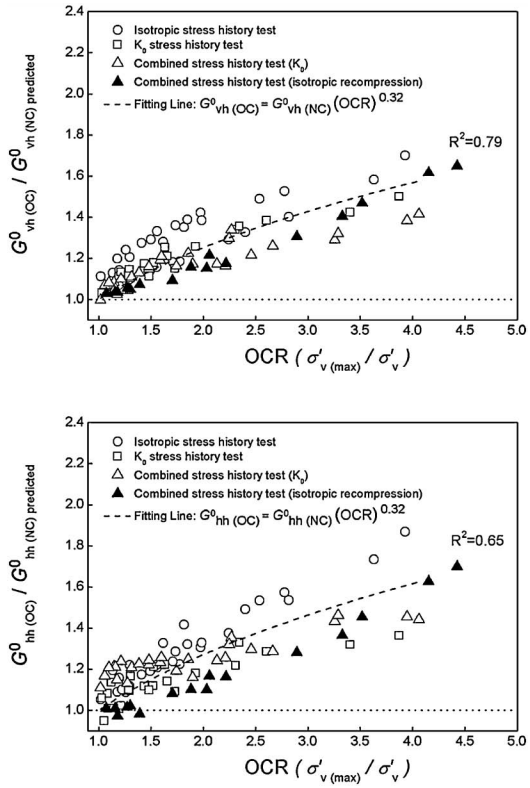

Fig. 9. $G^0_{(OC)}/G^0_{(NC)}$ for various values of the OCR: (a) G^0_{vh}; (b) G^0_{hh}

Figure 8 shows the variation of the initial stiffness normalized by the power functions of the vertical and horizontal stresses. The exponent has been previously derived from the data in the NC state and is given in Eqs. (4) to (7). Both normalized G^0_{vh} and G^0_{hh} for the normally consolidated soils remain constant for a variety of vertical stresses. For overconsolidated soils, the normalized stiffness increases as the vertical stress decreases and the corresponding OCR increases. Considering the previous discussion on Fig. 7, therefore, an OCR function should be employed to properly describe the variation of the initial stiffness of overconsolidated soils.

The OCR function can be obtained using the ratios of the initial stiffness of the overconsolidated soil to that of the normally consolidated soil under the same stress conditions. For a given stress state, the initial stiffness of the normally consolidated soil can be evaluated selectively using Eqs. (4), (5), (6), or (7) with respect to the loading program. Figure 9 shows the ratios, $G^0_{vh(OC)}/G^0_{vh(NC)}$ and $G^0_{hh(OC)}/G^0_{hh(NC)}$, plotted against the OCR value. As the OCR increases, both ratios generally increase with a fairly wide scattering. Similar variations are observed for both the K_0 stress history test and the primary K_0 loading of combined stress history test because both loadings were conducted under essentially the same K_0 stress condition. The ratios for the isotropic stress history test are in the upper bound of the range, while the ratios for the isotropic recompression of the combined stress history test are in the lower bound. This implies that even under the same isotropic stress condition and for the same OCR value, the initial stiffness cannot be normalized completely, but is influenced by the previous history of the stress ratio. At the present time, unfortunately, there is insufficient experimental data to confirm the dependency of the initial stress on the stress-ratio history. In this study, only the stress history recorded by the OCR values to predict the initial stiffness was considered.

A power law relationship between the OCR and initial stiffness, $(OCR)^k$, was obtained using a least-square regression. The exponent, k, is approximately 0.32 for both $G^0_{vh(OC)}/G^0_{vh(NC)}$ and $G^0_{hh(OC)}/G^0_{hh(NC)}$. It is worth noting that in the range of the OCR between 1.0 and 1.5, the value of $G^0_{hh(OC)}/G^0_{hh(NC)}$ in the isotropic recompression of the combined stress history test oscillates around 1.0, which indicates that the OCR has little effect on the initial horizontal stiffness in the low degree of overconsolidation. The value of $G^0_{hh(OC)}/G^0_{hh(NC)}$ starts to increase more slowly in the isotropic recompression of the combined stress history test than in other tests.

The anomaly in $G^0_{hh(OC)}$ observed in the isotropic recompression of the combined stress history test appears trivial in comparison with the wide scattering of the measured values, but it is still worth investigating a reason for this response.

Figure 10 shows a schematic diagram of the stress-void ratio curve to explain the reciprocal relationship between the OCR and void ratio. Let a normally consolidated soil be unloaded from a stress point, C, in Fig. 9. During un-

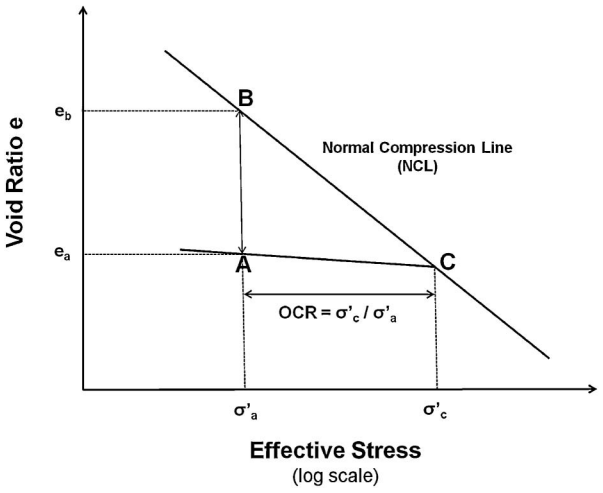

Fig. 10. Illustrative effective stress—void ratio relationship of clay

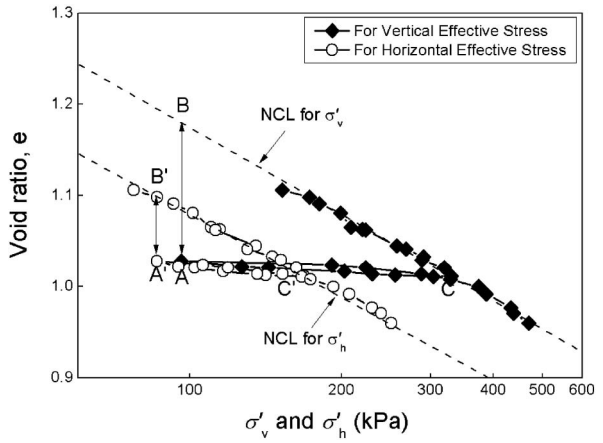

Fig. 11. Effective stress—void ratio relationship during the combined stress history test

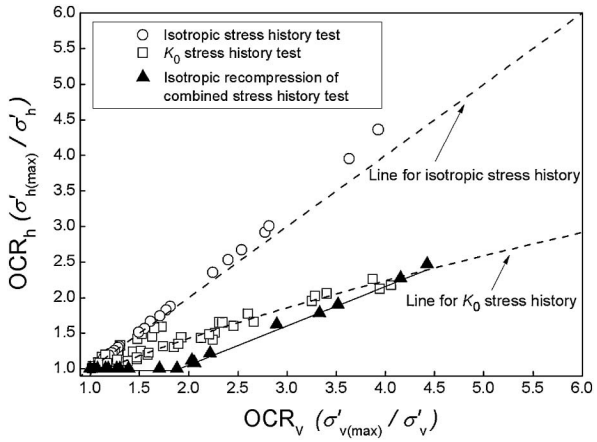

Fig. 12. Relationship between OCR_v and OCR_h for the three stress history tests

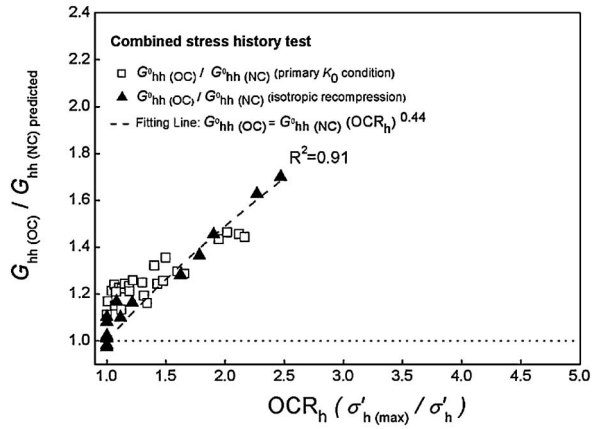

Fig. 13. $G_{hh(OC)}/G_{hh(NC)}$ of the combined stress history test with the OCR_h

loading, the particle packing does not change as much as in the previous virgin compression, i.e., under the normally consolidated condition. Consequently, at a given stress, the soil density, and thus initial stiffness, is higher in the overconsolidated state than in the normally consolidated state. As shown in Fig. 10, the difference in the void ratio between the overconsolidated and normally consolidated soils at the same stress level (i.e., line AB) is proportional to the relative distance between A and C, or the OCR value. That is, the effect of the OCR on the initial stiffness can be measured approximately by the magnitude of the difference in the void ratios of OC and NC soils at the same stress.

Figure 11 shows the variation of the void ratio plotted against both the vertical and horizontal effective stresses in the combined stress history. Initially, the soil is consolidated under the K_0 stress condition so that each point of the void ratio moves along the corresponding normally consolidated line (NCL). From points C and C′, the soil is unloaded under the K_0 stress condition until both vertical and horizontal stresses become identical at points A and A′, respectively. In the subsequent isotropic recompression, the point indicating the the void ratio moves along the recompression line, producing minor changes in the void ratio. During isotropic recompression, the line AB for the vertical stress (the void ratio difference between NCL and recompression line due to vertical stress change) is longer than the line A′B′ for the horizontal stress (the void ratio difference between NCL and recompression line due to horizontal stress change) so that the OCR is more influential in terms of the vertical stress than the horizontal stress. Therefore, the OCR in terms of the horizontal stress is more appropriate for describing small variations of $G^0_{hh(OC)}/G^0_{hh(NC)}$ in the isotropic recompression than the OCR in terms of vertical stress. To distinguish different stress components in defining the OCR, the notation of OCR_h as a ratio of the consolidation yield stress in the horizontal direction to current horizontal stress was introduced. In addition, OCR_v was employed instead of the conventional use of OCR for the vertical stress.

Figure 12 compares the variations of OCR_v and OCR_h in the three different loading programs. In the isotropic and K_0 stress history tests, a linear relationship between OCR_v and OCR_h can be observed. In the isotropic recom-

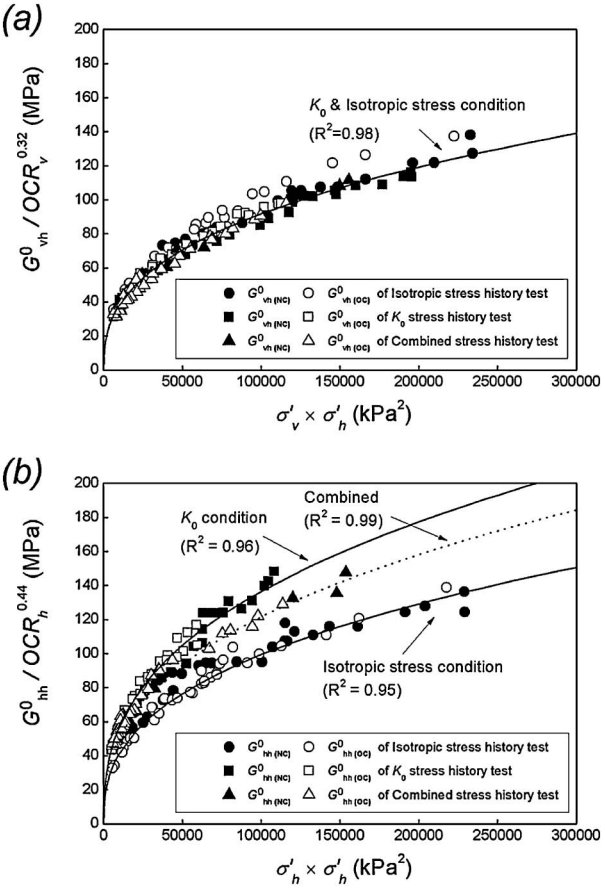

Fig. 14. Initial stiffness normalized by the power function of the OCR plotted against the vertical and horizontal stresses

pression of the combined stress history test, however, the linear relationship is only observed in the range of OCR_v between 2.0 and 4.5, while the OCR_h remains 1.0 in the OCR_v between 1.0 and 2.0. This implies that when a soil experiences a non-monotonic stress history, e.g., the combined stress history, the initial stiffness of the soil can be influenced by the directional stress history.

The anomaly of G^0_{hh} in Fig. 8(b) can be improved by introducing the OCR_h to the relationship between the anisotropic initial stiffness and the directional stress history. Figure 13 shows that the relationships of G^0_{hh} for the different loading programs essentially collapse into one, representing a unique relationship between $G^0_{hh(OC)}/G^0_{hh(NC)}$ and OCR_h. A power law relationship with the exponent of 0.44 quite accurately describes the dependence of G^0_{hh} on the horizontal stress history. Figure 14 presents variations of the initial stiffness normalized by the OCR function. The normalized initial stiffness of the overconsolidated soils exhibits the same pattern for the normally consolidated soils, thus properly accounting for the effect of the directional stress history.

CONCLUSIONS

An experimental study using triaxial stress tests with bi-axial bender element measurement was conducted on specimens obtained from reconstituted kaolinite samples to investigate the anisotropic initial stiffness under isotropic, K_0 and combined stress history conditions. Based on the results and analyses of the data, the following conclusions are drawn related to the effect of the directional stress history on the anisotropy of the initial shear stiffness of cohesive soil.

(1) The empirical correlation of the initial stiffness, which was established based on the data for normally consolidated soils, is valid for G^0_{vh}. However, a unique relationship between the initial horizontal stiffness, G^0_{hh}, and the horizontal stress cannot be attained, but the relationship depends on the stress ratio and previous stress history.

(2) The OCR function is necessary in the empirical correlation of the initial stiffness to properly consider the effect of the stress history on the initial stiffness of overconsolidated clay. The power law relationship of the OCR describes the dependency of G^0_{vh} on the stress history well. However, the values of $G^0_{hh(OC)}$ normalized by $G^0_{hh(NC)}$ do not show a single linear pattern against the conventional OCR values.

(3) The effect of the stress history on G^0_{hh} can be properly considered by defining the degree of overconsolidation in terms of horizontal effect stress, OCR_h.

ACKNOWLEDGEMENTS

The authors thank Young-Joo Ko and Choong-Hyun Lee for their assistance of this study. Financial support for this work was provided by Research Institute of Construction and Environmental Engineering in Seoul National University, Korea Institute of Construction Technology (KICT), and National Research Foundation of Korea (NRF) grant funded by the Korean government (MEST) (No. 2010-0015189).

REFERENCES

1) Bellotti, R., Jamiolkowski, M., LoPresti, D. C. F. and Oneill, D. A. (1996): Anisotropy of small strain stiffness in Ticino sand, *Geotechnique*, **46**(1), 115–131.
2) Clayton, C. R. I. and Heymann, G. (1999): Stiffness of geomaterials from small strain triaxial and field geophysical tests, *Proceedings of the Second International Symposium on Pre-failure Deformation Characteristics of Geomaterials*, Torino, 65–71.
3) Gasparre, A., Nishimura, S., Minh, N. A., Coop, M. R. and Jardine, R. J. (2007): The stiffness of natural London Clay, *Geotechnique*, **57**(1), 33–47.
4) Hardin, B. O. and Richart, F. E. J. (1963): Elastic wave velocities in granular soils, *Journal of Soil Mechanics and Foundation Engineering*, ASCE, **89**(SM1), 33–65.
5) Hardin, B. O. (1978): The nature of stress-strain behavior for soils, *Earthquake Engineering and Soil Dynamics, Proc. ASCE Geotech, Div. Spec. Conf.*, Pasadena, Calif., 3–90.
6) Hardin, B. O. and Kalinski, M. E. (2005): Estimating the shear modulus of gravelly soils, *Journal of Geotechnical and Geoenvironmental Engineering*, **131**(7), 867–875.
7) Hoque, E. and Tatsuoka, F. (2004): Effects of stress ratio on small-strain stiffness during triaxial shearing, *Geotechnique*, **54**(7), 429–439.
8) Jamiolkowski, H., Lancellotta, R. H. and Lo Presti, D. C. F.

(1995): Remarks on the stiffness at small strains of six Italian clays, *Proc. 1st Int. Symp. on Pre-failure deformation of geomaterials*, 817–836.
9) Jardine, R. J. (1995): One perspective of the pre-failure deformation characteristics of some geomaterials, *Pre-failure Deformation of Geomaterials*, Shibuya, (eds. by Mitachi, and Miura), 855–885.
10) Kim, C.-Y. (2004): Newly developed approach of stress path method for rational settlement estimation of saturated clay deposits, *Ph.D thesis*, Seoul National University, Seoul.
11) Kuwano, R. and Jardine, R. J. (2002): On the applicability of cross-anisotropic elasticity to granular materials at very small strains, *Geotechnique*, **52**(10), 727–749.
12) Lee, J. S. and Santamarina, J. C. (2005): Bender elements: Performance and signal interpretation, *Journal of Geotechnical and Geoenvironmental Engineering*, ASCE, **131**(9), 1063–1070.
13) Lings, M. L., Pennington, D. S. and Nash, D. F. T. (2000): Anisotropic stiffness parameters and their measurement in a stiff natural clay, *Geotechnique*, **50**(2), 109–125.
14) Mitaritonna, G., Amorosi, A. and Cotecchia, F. (2008): Elastic stiffness anisotropy of clay samples radially compressed along different stress ratio triaxial paths, *Deformation Characteristics of Geomaterials*, (eds. by Burns, Mayne, and Santamarina), IOS Press, Atlanta, U.S.A., 589–595.
15) Pennington, D. S., Nash, D. F. T. and Lings, M. L. (1997): Anisotropy of G_0 shear stiffness in Gault Clay, *Geotechnique*, **47**(3), 391–398.
16) Rampello, S., Viggiani, G. M. B. and Amorosi, A. (1997): Small-strain stiffness of reconstituted clay compressed along constant triaxial effective stress ratio paths, *Geotechnique*, **47**(3), 475–489.
17) Santagata, M., Germaine, J. T. and Ladd, C. C. (2005): Factors affecting the initial stiffness of cohesive soils, *Journal of Geotechnical and Geoenvironmental Engineering*, ASCE, **131**(4), 430–441.
18) Santagata, M. (2008): Effects of stress history on the stiffness of a soft clay, *Deformation Characteristics of Geomaterials*, (eds. by Burns, Mayne, and Santamarina), IOS Press, Atlanta, USA, 95–123.
19) Viggiani, G. and Atkinson, J. H. (1995): Stiffness of fine-grained soil at very small strains, *Geotechnique*, **45**(2), 249–265.